magnetochemistry

MDPI

Article

A Dy^{III} Complex of a Pentadentate Schiff Base with Field-Induced Single-Ion Magnet Behaviour

Julio Corredoira-Vázquez [1,2,*], Paula Oreiro-Martínez [1], Ana M. García-Deibe [1], Jesús Sanmartín-Matalobos [1,3] and Matilde Fondo [1,*]

1 Departamento de Química Inorgánica, Facultade de Química, Universidade de Santiago de Compostela, Campus Vida, 15782 Santiago de Compostela, Spain
2 Phantom-g, CICECO—Aveiro Institute of Materials, Department of Physics, University of Aveiro, 3810-193 Aveiro, Portugal
3 Institute of Materials (iMATUS), Universidade de Santiago de Compostela, 15782 Santiago de Compostela, Spain
* Correspondence: julio.corredoira.vazquez@usc.es (J.C.-V.); matilde.fondo@usc.es (M.F.)

Abstract: The influence of the solvent in the reaction of dysprosium(III) chloride hydrate with the N_3O_2 ligand H_2L (2,6-bis(2-hydroxyphenyliminomethyl)pyridine) was studied To this end, the new mononuclear chloride complex $[Dy(L)Cl(H_2O)_2]$ (**1**) was isolated in absolute ethanol as solvent, without any evidence of the hydrolysis of the ligand. This clearly contrasts with previous results, where a similar reaction in methanol proceeds with the partial hydrolysis of the Schiff base, and the formation of a new hemiacetal donor to yield $[Dy(HL')_2)][Dy(L)(Cl_2)]$ (H_2L' = (6-(2-hydroxyphenyliminomethyl)-2-methoxyhydroxymethyl)pyridine). The single crystal X-ray structure of the chloride complex **1** shows that the Dy^{III} ion is octacoordinated in a highly distorted N_3O_4Cl environment between triangular dodecahedral and biaugmented trigonal prisms. The full magnetic characterisation of **1** shows that it presents field-induced single ion magnet behaviour, with a thermal energy barrier U_{eff} of 113.5 K, which is the highest among dysprosium complexes derived from H_2L.

Keywords: dysprosium; single ion magnet; N_3O_2 pentadentate ligand; Schiff base; chloride ligand

Citation: Corredoira-Vázquez, J.; Oreiro-Martínez, P.; García-Deibe, A.M.; Sanmartín-Matalobos, J.; Fondo, M. A Dy^{III} Complex of a Pentadentate Schiff Base with Field-Induced Single-Ion Magnet Behaviour. *Magnetochemistry* **2023**, *9*, 62. https://doi.org/10.3390/magnetochemistry9030062

Academic Editor: Salah Massoud

Received: 29 January 2023
Revised: 16 February 2023
Accepted: 20 February 2023
Published: 23 February 2023

1. Introduction

Single-molecule magnets (SMMs), and within them, single-ion magnets (SIMs), which are quantum in nature, are at the vanguard of new technological developments in spintronics and quantum information processing [1,2]. This is because the properties of these magnets are inherent to the molecule, enabling an extraordinary degree of device miniaturization. Moreover, the molecular nature of these systems offers the possibility of introducing different functionalities into the devices, which is a great additional advantage. However, there are still many challenges to overcome before molecule magnets can be used at a technological level. The first commitment is to obtain SMMs that remain stable in air with higher blocking temperatures than has been achieved so far. The up-to-date record blocking temperature (T_B) is 80 K, and it is held by the SIM $[(Cp^{iPr5})Dy(Cp^*)][B(C_6F_5)$ [3], a similar T_B to that recently achieved by a dinuclear mixed-valent dysprosium metallocene [4]. Therefore, the T_B of these compounds exceeds the temperature of liquid nitrogen, which allows a glimpse of the use of these magnets in nanotechnology. However, a major drawback of these metallocenes is that they are unstable in air. Consequently, the field of molecular magnets is still wide open, and obtaining air-stable coordination compounds with geometries that can improve the anisotropy of the systems, and, accordingly, their functioning, is an area of growing interest. In this way, some air stable complexes of oblate ions with highly axial D_{5h} symmetry, mainly derived from phosphine oxides and other auxiliary monodentate ligands [5–7], have been reported to show high anisotropy, and, consequently,

good magnetic performance, with blocking temperatures of up to 20 K [5]. However, isolating compounds with a predetermined geometry from monodentate ligands is not an easy task, and obtaining a specific geometry often rather seems to be the result of serendipity. Therefore, a more rational strategy to predetermine highly axial geometries around oblate ions should be the use of rigid ligands that occupy the equatorial plane, and to fill the apical positions with monodentate ancillary donors. This is an emerging approach and, in this way, dysprosium compounds with fairly rigid macrocyclic ligands are beginning to show promising results [8]. However, the field of rigid acyclic ligands seems poorly explored [9–12], where results so far have been mixed. In this specific field, we began to study the coordination capability of a previously well-known air-stable pentadentate Schiff base, H_2L (Scheme 1) [13], with Dy^{III} ions [14], and accordingly, we have published the first lanthanoid coordination compounds with this type of ligand, many of which show slow relaxation of the magnetization. However, in this reported study [14], we were unable to obtain a dysprosium complex with the non-hydrolysed Schiff base and chloride as auxiliary donor. As a continuation of this work, the effect of the synthesis solvent on the complexes to be obtained was studied, and thus the new compound $[Dy(L)Cl(H_2O)_2]$ (**1**), whose behaviour as a magnet is also analysed, was able to be isolated and it is presented herein.

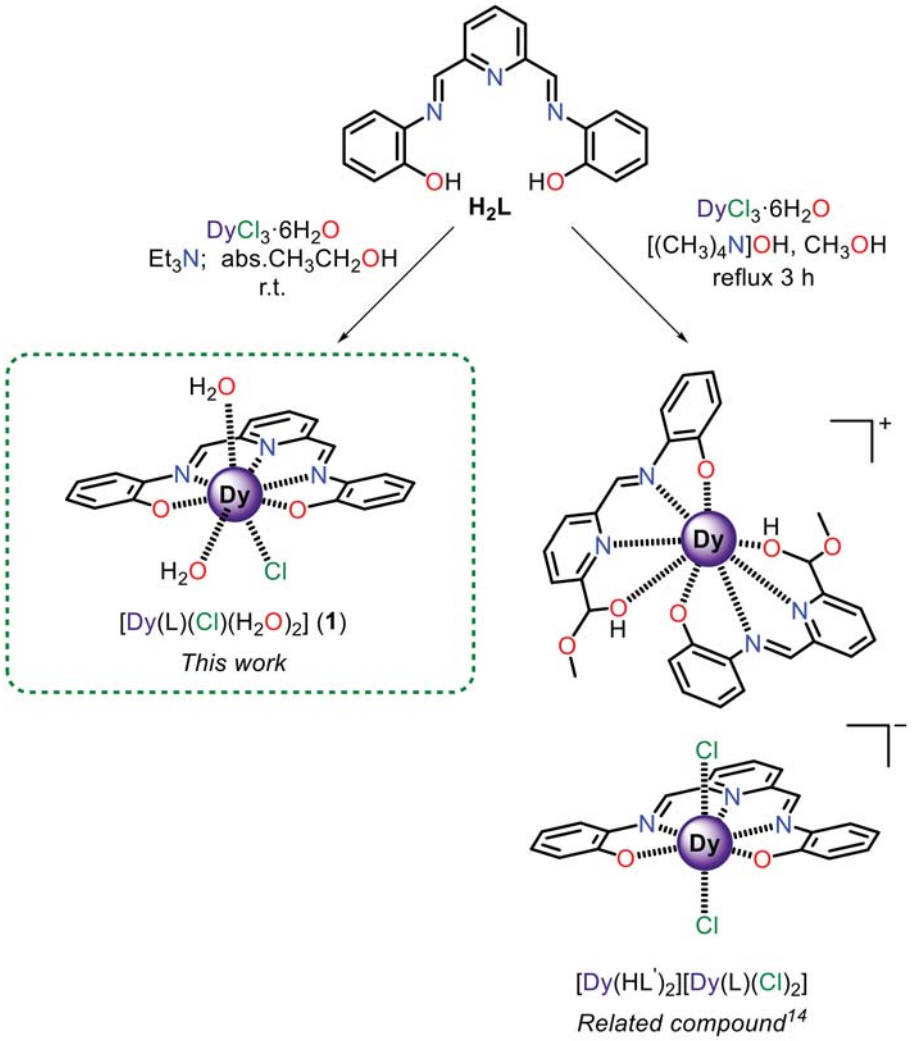

Scheme 1. Synthetic route for the isolation of **1** and the related complex $[Dy(HL')_2][Dy(L)(Cl_2)]$ [14].

2. Results and Discussion

2.1. Synthesis

The reaction of $DyCl_3 \cdot 6H_2O$ at room temperature with an absolute ethanol solution of H_2L, basified with triethylamine, leads to the isolation of the molecular mononuclear complex $[Dy(L)Cl(H_2O)_2]$ (**1**), whereas a similar related reaction in methanol at reflux yields the dinuclear ionic compound $[Dy(HL')_2)][Dy(L)(Cl_2)]$, as shown in Scheme 1 [14].

In view of these results, it might seem that there are two factors that can affect the obtaining of the different compounds by favouring the hydrolysis of the H_2L ligand: the solvent of the reaction and the temperature. Thus, in order to discern which of the two factors promotes Schiff base cleavage, the same reaction leading to **1** was repeated at reflux temperature, and it yields the same complex. In addition, further evidence that temperature does not seem to influence the cleavage of the Schiff base is that similar complexes with nitrate [14] instead of chloride as an ancillary donor have also been obtained in 96% ethanol at reflux, without any sign of the hydrolysis of the ligand. Therefore, it appears that the temperature plays no role in the hydrolysis process, but that the solvent is crucial, this process being highly favoured for methanol. In principle, this could be attributed to the higher amount of water present in methanol compared to the absolute ethanol (98%) used in the synthesis of **1**. However, this does not seem to be a determining factor, considering that dysprosium complexes containing H_2L and nitrate as ligands were able to be obtained from 96% ethanol solutions [14], and that the starting salts for the syntheses are always hydrated. Therefore, perhaps the slightly more acidic character of methanol over ethanol could contribute to the easier hydrolysis in methanolic solution.

Complex **1** is a deep red solid, which is air stable and does not lose water ligands, at least not at temperatures slightly above 100 °C (ca. 125 °C). The complex was completely characterized by means of elemental analysis, infrared spectroscopy, and single and powder X-ray diffraction studies. In addition, the full magnetic characterization of the sample and its behaviour as a magnet were also analysed.

The IR spectrum of compound **1** (Figure S1) shows two sharp bands located at 1533 and 1583 cm^{-1}, which could be assignable to the ν(C=N) vibrations of the pyridine and imine bonds [14], respectively. These bands experience negative displacements with relation to the ones of the free H_2L, and this shift agrees with the coordination of both the pyridine and imine nitrogen atoms to the dysprosium metal ion. In addition, a broad band centred at 3315 cm^{-1} is in agreement with the existence of water coordinated to the metal atom.

2.2. X-ray Diffraction Studies

Figure 1 shows an ellipsoid diagram for complex **1**, and the main distances and angles regarding the dysprosium ion for this compound are summarised in Table S1.

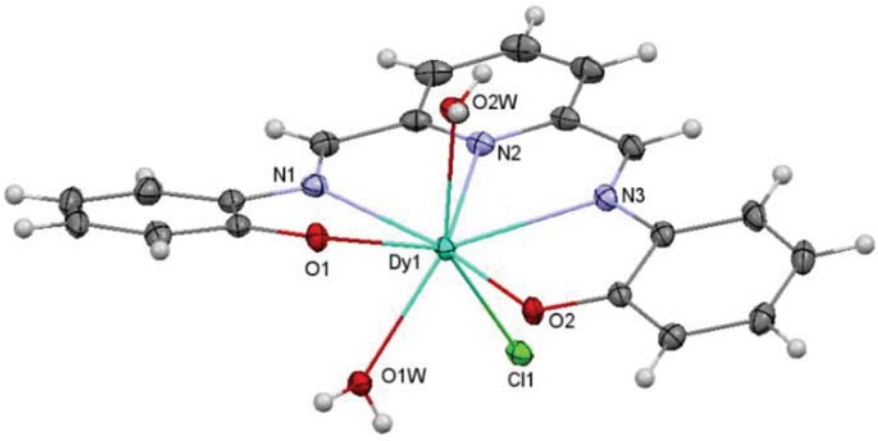

Figure 1. Ellipsoid diagram for **1** at 50% probability.

The asymmetric unit of **1** just contains neutral [Dy(L)Cl(H_2O)$_2$] molecules, without any solvate. In the [Dy(L)Cl(H_2O)$_2$] complex, both phenol oxygen atoms of the Schiff base are deprotonated. This dianionic L^{2-} base acts as a pentadentate N_3O_2 ligand, using all its potential donor atoms. Despite the conjugation of the deprotonated ligand, which should make it practically flat, it adopts a helical arrangement in this complex, as was observed in certain previously described complexes of this donor [14].

Consequently, O1 and O2 are the most protruding atoms from the mean N_3O_2 computed plane, which are ca. 0.35 Å above or below this plane. The dysprosium ion is also out ofthe calculated plane, from where it protrudes ca. 0.39 Å.

The coordination sphere of the Dy^{III} ion is fulfilled by three further monodentate ligands: two water molecules and a chloride anion. Hence, the Dy^{III} ion has coordination number 8, with an N_3O_4Cl environment. The calculations of the grade of distortion of the DyN_3O_4Cl core relative to an ideal polyhedron of eight vertexes with the SHAPE program [15] reveals a largely distorted geometry between a biaugmented trigonal prism and a triangular dodecahedron (Table S2). The main angles and distances of the dysprosium ion (Table S1) are comparable to those previously reported for this kind of compound [10,14,16], and do not deserve further consideration.

Finally, the mononuclear units [Dy(L)Cl(H_2O)$_2$] establish hydrogen bonds among them, involving both water and chloride ligands. These interactions expand the initial mononuclear block in a zigzag chain, as shown in Figure 2, and this leads to the shortest intermolecular distance between Dy^{III} ions being 5.4407(7) Å.

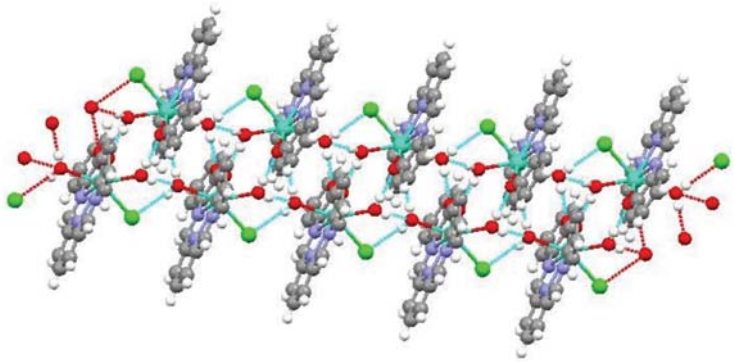

Figure 2. Hydrogen bond scheme for **1**, showing the zig-zag chain arrangement.

Moreover, powder X-ray diffraction measures for the raw sample of **1** (Figure S2) were performed. These studies show that the bulk sample of the isolated product and the solved single crystals are the same complex, and that it has been obtained with high purity, given that no other peaks can be observed in the experimental diffractogram.

2.3. Magnetic Properties

The temperature change in magnetic susceptibility data for [Dy(L)Cl(H_2O)$_2$] (**1**) was registered. Figure 3 represents the $\chi_M T$ product vs. T.

The value of this $\chi_M T$ product at 300 K is 14.42 cm^3Kmol^{-1}, which is very similar to the calculated one for an isolated Dy^{3+} ion (14.13 cm^3Kmol^{-1}). This $\chi_M T$ value remains virtually constant when the temperature drops to 35 K, and then it diminishes to 2 K, touching a minimum value of 9.71 cm^3kmol^{-1}. This fall in the curve can be attributed primarily to the depopulation of the M_J sublevels of the Dy^{III} ion at low temperatures, although it cannot be ruled out that antiferromagnetic intermolecular interactions also contribute to this drop.

The value of reduced magnetisation at 2 K points to 5.58 $N\mu_B$ at the highest applied field of 50,000 Oe (see Figure 3 inset). This value is much less than that calculated for a Dy^{III} ion with $g = 4/3$ and $J = 15/2$ (10 $N\mu_B$), but it is quite close to the value of a largely anisotropic Dy^{III} ion with an Ising-like ground doublet (5 $N\mu_B$) [17]. Accordingly, both

the susceptibility and reduced magnetisation measurements seem to agree with a quite anisotropic system.

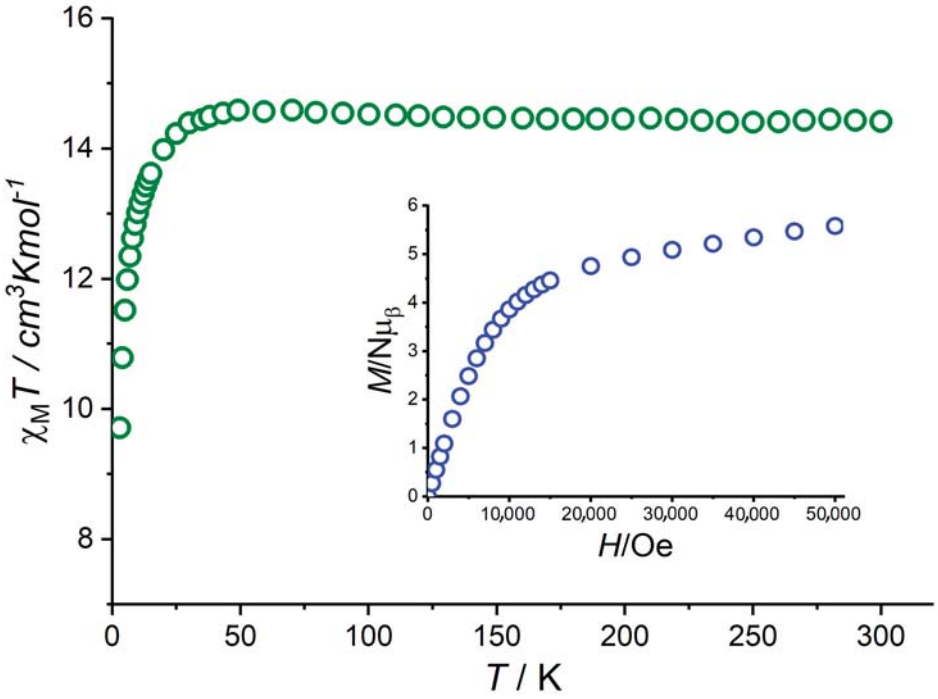

Figure 3. $\chi_M T$ vs. T graph for **1**. Inset: $M/N\mu_B$ vs. H at 2 K.

In the light of these results, the low-temperature magnetic relaxation behaviour of this complex was also studied. Accordingly, alternating current (ac) magnetic susceptibility data were registered at a frequency of 8000 Hz in a zero dc external field. Under these conditions, no in-phase (χ'_M) or out-of-phase ac susceptibility (χ''_M) peaks were observed (Figure S3). This could be because the relaxation of the magnetisation is extremely fast, or because there is a substantial quantum tunnelling of the magnetisation (QTM) [18,19]. A common way to see whether quantum tunnelling exists is to apply an external dc magnetic field [20], as this would destroy the bistability of the ground state, and thus the possibility of the quantum tunnel effect. Therefore, different static magnetic fields were applied in order to see whether they were able to remove the QTM with the aim of establishing the optimum field. Consequently, new ac susceptibilities as a function of the temperature were recorded under the presence of various dc fields, which allowed the establishment of an optimal field of 1500 Oe (Figure S4). Hence, new ac susceptibility data were again recorded under this dc field (χ'_M in Figure S5 and χ''_M in Figure 4). In these conditions, χ''_M (Figure 4) peaks between 4.5 and 8 K at different fixed frequencies (ranging between 10 and 10,000 Hz) can be observed.

Moreover, the Cole–Cole graph for **1** (Figure S6) shows semicircles with α parameters extracted using a generalised Debye model (Table S3) that range from 0.22 to 0.12. These α values seem to indicate that many relaxation processes are operative at low temperatures.

In addition, studies on the relaxation of the magnetization were additionally performed by examining the dependence of relaxation time (τ) on the temperature. Thus, the representation of the variation of τ with the temperature (Arrhenius plot, Figure 5) shows a deviation from linearity at the low-temperature region, and this, in combination with the α parameters obtained from the Cole–Cole graph, indicates that the line cannot be replicated with an Orbach relaxation model alone.

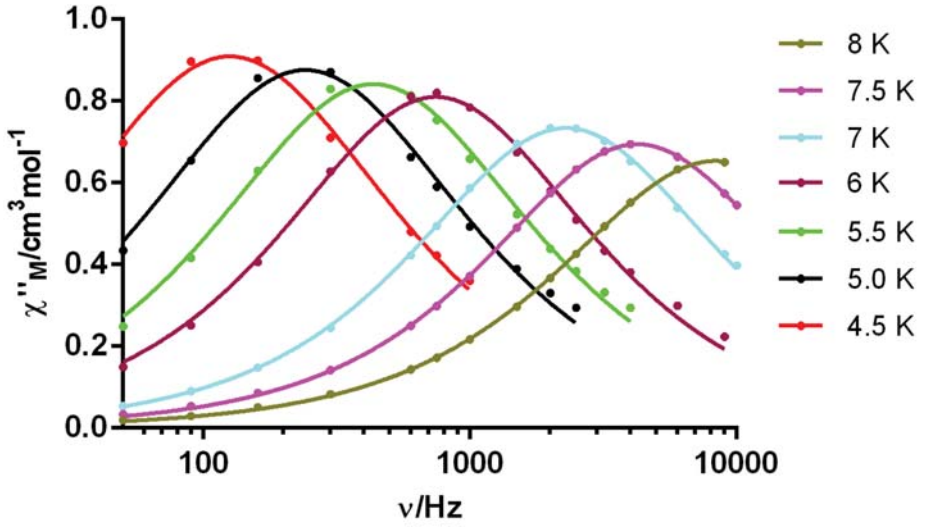

Figure 4. Variation of χ''_M with the frequency for **1** under a dc external field of 1500 Oe at temperatures ranging between 4.5 and 8 K.

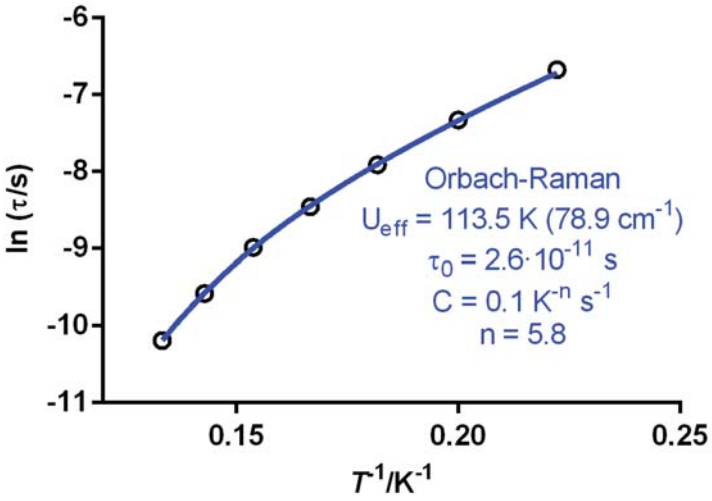

Figure 5. Arrhenius graph for **1** under an external dc applied field of 1500 Oe. The blue line represents the best fit, taking into account Orbach plus the Raman relaxation processes (Equation (1)).

Therefore, many efforts were made to reproduce this graph, taking into consideration all the possible relaxation processes (Orbach, Direct, Raman, and QTM). Thus, the fit that best replicated this plot with rational parameters considering all these processes, individually or grouped, was obtained using Orbach and Raman relaxation (Equation (1)), and the different attempts at fitting the curve including the QTM relaxation process were all unsuccessful. This mentioned fit renders an energy barrier for the reversal of the magnetization of 113.5 K, with a τ_0 factor of 2.6×10^{-11} s, and Raman values of C = 0.1 $K^{-n}s^{-1}$ and $n = 5.8$. This n value could seem much lower than anticipated for a Dy^{III} ion ($n = 9$), but the implication of acoustic and optical phonons in magnetic dynamics can justify the divergence from the foreseen value for a Dy^{III} Kramers ion [21,22]. In fact, this value lies between the range of 5 and 9 usually reported for several other dysprosium complexes [23].

$$\tau^{-1} = CT^{-n} + {\tau_0}^{-1}e^{-U_{eff}/k_BT} \quad (1)$$

In an attempt to deepen the understanding of the magnetic behaviour, the anisotropy axis of the dysprosium ion was calculated using the MAGELLAN program [24] (Figure 6,

left). Thus, it can be seen that the anisotropy axis is practically aligned with the Dy-O1 bond. Accordingly, the anisotropy axis of **1** coincides with the geometric axial axis of a biaugmented trigonal prism (Figure 6, right). Therefore, this marks an axiality that justifies that the compoundbehaves like a molecule magnet. However, the hydrogen bond interactions present in this complex (see crystallographic discussion) could enhance the quantum tunnelling of the magnetization and, as a result, avoid the observation of molecule magnet behaviour in the absence of an external magnetic field, as has already been demonstrated for other dysprosium compounds with the same ligand [14]. In spite of this, the U_{eff} barrier for **1** is the highest among the reported dysprosium complexes derived from H_2L (Table S4). It must be noted that all of the previously published non-ionic Dy^{III} compounds with this Schiff base ligand show the coordination number 9, while in complex **1**, the dysprosium ion is in an octacoordinated environment. Consequently, it seems that the use of monodentate ligands instead of potentially bidentate ones (chloride instead of nitrate) decreases the coordination number, which seems to be accompanied by an increase in the energy barrier. However, given the different coordination numbers, which lead to very different geometries, it is not possible to establish further magneto-structural correlations.

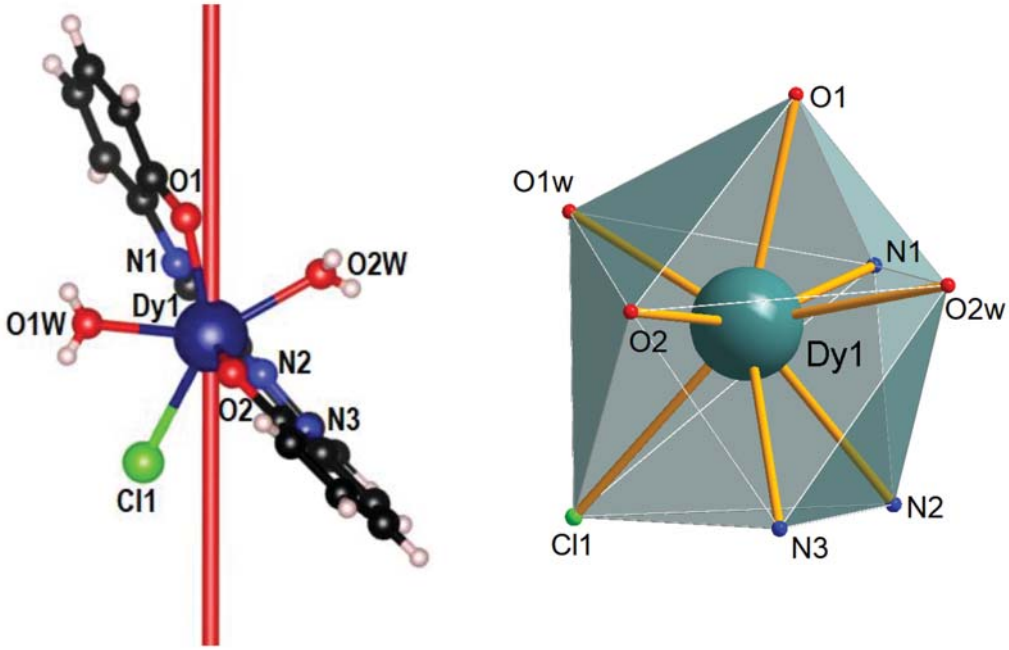

Figure 6. (**Left**) Calculated orientation of the local main magnetic axis (red) on Dy^{III} ion for **1** using MAGELLAN software [24]. (**Right**) Coordination polyhedra for de Dy^{III} ion in **1**, showing O1 at the apex of the distorted biaugmented trigonal prism environment.

In addition, the energy barrier for the spin reversal in **1** was compared with the one of other dysprosium complexes with other rigid N_3O_2 ligands. Not many complexes of this kind were found, and, to our knowledge, the only other planar rigid ligands that behave as N_3O_2 donors are hydrazones, all of which are derived from 2,6-diacetylpyridine and various hydrazides. The comparison of U_{eff} in **1** and in these Dy^{III} complexes derived from hydrazones under different magnetic fields shows that **1** still remains the compound with the highest energy barrier for the reversal of magnetization among those with a predetermined quasi-planar equatorial N_3O_2 environment and coordination numbers 8 [8,25] or 9 [10,26].

3. Materials and Methods

3.1. Materials and General Methods

All the chemical reagents used in the present work were purchased from trading houses, and they were used as supplied by the provider, without additional purification.

The elemental analyses of C, H, and N for the Schiff base H_2L, and for the dysprosium complex **1** were performed on a Themoscientific Flash Smart analyser. The infrared spectrum of **1** was registered between 4000 and 500 cm^{-1} on a Varian 670 FT/IR spectrophotometer operating in the ATR mode. A Varian INNOVA-400 spectrometer was used to record the ^1H NMR spectrum of H_2L in the DMSO-d_6 as solvent.

3.2. Syntheses

The well-known H_2L ligand was obtained via the modification of a method previously described [13], as published by us [14], and adequately characterized in solid state by elemental analysis, and in solution by ^1H NMR spectroscopy.

[Dy(L)(Cl)$(H_2O)_2$] (**1**): a solution of $DyCl_3 \cdot 6H_2O$ (0.130 g, 0.347 mmol) in absolute ethanol (10 mL) was added to a solution of a mixture of H_2L (0.110 g, 0.347 mmol) and Et_3N (0.095 g, 0.941 mmol) in absolute ethanol (35 mL). This mix was stirred at room temperature for 3 h, and the small quantity of solid formed was separated by centrifugation and discarded. The obtained solution was filtered to remove any possible impurities, and then it was allowed to steadily evaporate until single crystals of [Dy(L)(Cl)$(H_2O)_2$] (**1**), suitable for X-ray diffraction studies, were obtained. The single crystals were filtered, and then dried in an oven. Yield: 0.072 (58%). Elemental analysis calcd. for $C_{19}H_{17}DyN_3O_4Cl$ (549.31): C 41.54, N 7.65, H 3.12%. Found: C 42.11, N 7.68, H 3.41%. IR (ATR, $\tilde{\nu}/cm^{-1}$): 1533 (νCN_{py}), 1583 (νCN_{imine}), 3315 (νOH).

The same compound was isolated when this reaction was repeated exactly with the same quantity of reactants and solvents but heating at reflux. Elemental analysis calcd. for $C_{19}H_{17}DyN_3O_4Cl$ (549.31): C 41.54, N 7.65, H 3.12%. Found: C 41.64, N 7.82, H 3.50%.

3.3. Single X-ray Crystallographic Refinement and Structure Solution

Table S5 summarises the crystal data and the details of the refinement for the crystal structure of the metal complex **1**. Single crystals of **1**, suitable for single X-ray diffraction analysis, were isolated as detailed previously. The data were recorded on a Bruker D8 VENTURE PHOTON III-14 diffractometer at a temperature of 100 K, using graphite monochromatised Mo-*Kα* (λ = 0.71073 Å) radiation. Multi-scan absorption corrections were carried out through the use of the SADABS routine [27]. The structure was resolved by means of standard direct methods, with the software SHELXT, and next refined by full matrix least squares techniques on F^2 by utilising SHELXL [28] from the program package SHELX-2018 [28]. The atoms that were different to hydrogen were anisotropically refined, whereas hydrogen atoms were normally included in the structure factor calculations in geometrically idealised positions. Hydrogen atoms bonded to oxygen atoms (water) were found in the Fourier map, with the aim of obtaining the hydrogen bond scheme. These atoms were freely refined in this case.

3.4. Powder X-ray Diffraction Studies

X-ray powder measurements for **1** were also performed. The powder X-ray diffraction data of **1** were registered on a Philips diffractometer, equipped with a "PW1710" type unit control, a vertical "PW1820/00" type goniometer, and an "Enraf Nonius FR590" type generator, functioning at 40 kV and 30 mA, using monochromatised radiation (Cu-Kα, λ = 1.5418 Å) radiation. A scan in the range $2 < 2\theta < 30^\circ$ was performed, with t = 3 s and $\Delta 2\theta = 0.02^\circ$. LeBail refinement was achieved with the help of HighScore Plus Version 3.0d.

3.5. Magnetic Measurements

Experimental magnetic susceptibility dc and ac measurements were recorded for a microcrystalline sample of **1** on a PPMS Quantum Design susceptometer. The dc magnetic susceptibility data were registered between 2 and 300 K, under a magnetic field of 1000 Oe. Magnetisation measurements at 2.0 K were also performed, in this case under magnetic fields in the range 0 to 50,000 Oe. Diamagnetic corrections for the data were assumed on the basis of Pascal's tables. Alternating current (ac) susceptibility measurements in

the temperature range 0–10 K in the absence of an external dc field (H_{dc} = 0), and at H_{dc} = 1500 Oe, were recorded in an oscillating alternating current field of 3.5 Oe, with ac frequencies varying from 50 to 10,000 Hz. ac susceptibility measurements were also collected at the fixed temperature of 5 K at different magnetic fields (500 Oe, 800 Oe, 1000 Oe, 1500 Oe, 2000 Oe, 2500 Oe, 3000 Oe, and 3500 Oe) and at frequencies ranging between 50 and 2000 Hz in order to determine the optimum field for eliminating the quantum tunnel of the magnetization.

4. Conclusions

The isolation of the neutral mononuclear complex [Dy(L)Cl(H_2O)$_2$] (**1**) was favoured over that of the related ionic compound [Dy(HL')$_2$)][Dy(L)(Cl_2)], in which the Schiff base was partially hydrolysed, simply by changing the methanol reaction solvent by absolute ethanol. Compound **1** behaves as a single ion magnet in the presence of an optimal external magnetic field of 1500 Oe, with an U_{eff} barrier of 113.5 K. This behaviour is promoted by the easy axis of the anisotropy, which points to the vertex of a biaugmented trigonal prism, rendering the highest barrier for the inversion of the magnetization among the scarcely reported mononuclear dysprosium complexes of H_2L, and the related Dy^{III} compounds with planar N_3O_2 hydrazones as ligands and coordination numbers 8 or 9. Therefore, this study presents a new example of a field-induced SIM with a rigid acyclic ligand, thus contributing to an increase in the knowledge of magnetic properties in this field where examples are still fairly scarce. Thus, **1** seems to show that the use of monodentate auxiliary ligands decreases the rate of coordination compared to ancillary bidentate ligands, so improving the energy barrier for magnetisation reversal.

Supplementary Materials: The following supporting information can be downloaded at: https://www.mdpi.com/article/10.3390/magnetochemistry9030062/s1: Table S1: Main bond distances (Å) and angles (º) for **1**. Table S2: SHAPE v2.1. Continuous Shape Measures Calculation (c) 2013 Electronic Structure Group, Universitat de Barcelona. Table S3: Generalised Debye model fitting parameters for **1**. Table S4: Comparison of certain structural and magnetic parameters for Dy^{III} complexes magneto-structurally characterised with the ligand H_2L. Table S5: Crystal data and structure refinement for **1**. Figure S1: IR spectrum for **1** in the 4000–500 cm^{-1} region. Figure S2: Comparative powder X-ray diffractograms for **1**. Figure S3: Left) Dependence of χ'_M on temperature for **1** at a frequency of 8000 Hz at H_{dc} = 0. Right) Dependence of χ''_M on temperature for **1** at a frequency of 8000 Hz at H_{dc} = 0. Figure S4: Left) Dependence of χ''_M on frequency for **1** at 5 K under various external applied fields. Right) Dependence of the magnetic relaxation time on field at 5 K for **1**. Figure S5: Dependence of χ'_M on frequency for **1** under H_{dc} = 1500 Oe between 4.5 and 8 K. Figure S6: Cole–Cole plot for complex **1** under an external field H_{dc} = 1500 Oe. CCDC 2238215 contains the supplementary crystallographic data for this paper. These data can be obtained free of charge via www.ccdc.cam.ac.uk/data_request/cif, by emailing data_request@ccdc.cam.ac.uk, or by contacting the Cambridge Crystallographic Data Centre, 12 Union Road, Cambridge CB2 1EZ, UK; Fax: +44-1223-336033.

Author Contributions: J.C.-V., investigation and conceptualization; P.O.-M., investigation; A.M.G.-D., methodology (X-ray diffraction studies); J.S.-M., supervision; M.F., conceptualization, supervision, and writing—original draft preparation and revision. All authors have read and agreed to the published version of the manuscript.

Funding: This research received no external funding. J.C.V. thanks Xunta de Galicia for his post-doctoral fellowship (ED481B-2022-068). P.O.M. thanks the Fundación Segundo Gil Dávila for her PhD fellowship.

Institutional Review Board Statement: Not applicable.

Informed Consent Statement: Not applicable.

Data Availability Statement: Data are contained within the article or Supplementary Materials.

Conflicts of Interest: The authors declare no conflict of interest.

References

1. Gaita-Ariño, A.; Luis, F.; Hill, S.; Coronado, E. Molecular spins for quantum computation. *Nat. Chem.* **2019**, *11*, 301–309. [CrossRef] [PubMed]
2. Moreno-Pineda, E.; Wernsdorfer, W. Measuring molecular magnets for quantum technologies. *Nat. Rev. Phys.* **2021**, *3*, 645–659. [CrossRef]
3. Guo, F.-S.; Day, B.M.; Chen, Y.-C.; Tong, M.-L.; Mansikkam-ki, A.; Layfield, R.A. Magnetic hysteresis up to 80 kelvin in a dysprosium metallocene single-molecule magnet. *Science* **2018**, *362*, 1400–1403. [CrossRef] [PubMed]
4. Gould, C.A.; McClain, K.R.; Reta, D.; Kragskow, J.G.C.; Marchiori, D.A.; Lachman, E.; Choi, E.-S.; Analytis, J.G.; Britt, R.D.; Chilton, N.F.; et al. Ultrahard magnetism from mixed-valence dilanthanide complexes with metal-metal bonding. *Science* **2022**, *375*, 198–202. [CrossRef] [PubMed]
5. Chen, Y.-C.; Liu, J.-L.; Ungur, L.; Liu, J.; Li, Q.-W.; Wang, L.-F.; Ni, Z.-P.; Chibotaru, L.F.; Chen, X.-M.; Tong, M.-L. Symmetry-supported magnetic blocking at 20 K in pentagonal bipyramidal Dy(III) single-ion magnets. *J. Am. Chem. Soc.* **2016**, *138*, 2829–2837. [CrossRef]
6. Li, L.-L.; Su, H.-D.; Liu, S.; Xu, Y.-C.; Wang, W.-Z. A new air- and moisture-stable pentagonal-bipyramidal Dy^{III} single-ion magnet based on the HMPA ligand. *Dalton Trans.* **2019**, *48*, 2213–2219. [CrossRef]
7. Gupta, S.K.; Dey, S.; Rajeshkumar, T.; Rajaraman, G.; Murugavel, R. Deciphering the role of anions and secondary coordination sphere in tuning anisotropy in Dy(III) air stable D_{5h} SIMs. *Chem. Eur. J.* **2022**, *28*, e202103585. [CrossRef]
8. Gil, Y.; Castro-Alvarez, A.; Fuentealba, P.; Spodine, E.; Aravena, D. Lanthanide SMMs based on belt macrocycles: Recent advances and general trends. *Chem. Eur. J.* **2022**, *28*, e202200336.
9. Singh, V.; Das, D.; Anga, S.; Sutter, J.-P.; Chandrasekhar, V.; Bar, A.K. Rigid N_3O_2-pentadentate ligand-assisted octacoordinated mononuclear Ln(III) complexes: Syntheses, characterization, and slow magnetization relaxation. *ACS Omega* **2022**, *7*, 25881–25890. [CrossRef]
10. Mondal, A.K.; Goswami, S.; Konar, S. Influence of the coordination environment on slow magnetic relaxation and photoluminescence behavior in two mononuclear dysprosium(III) based single molecule magnets. *Dalton Trans.* **2015**, *44*, 5086–5094. [CrossRef]
11. Bar, A.K.; Kalita, P.; Sutter, J.-P.; Chandrasekhar, V. Pentagonal-bipyramid Ln(III) complexes exhibiting single-ion-magnet behavior: A rational synthetic approach for a rigid equatorial plane. *Inorg. Chem.* **2018**, *57*, 2398–2401. [CrossRef] [PubMed]
12. Kalita, P.; Ahmed, N.; Bar, A.K.; Dey, S.; Jana, A.; Rajaraman, G.; Sutter, J.-P.; Chandrasekhar, V. Pentagonal bipyramidal Ln(III) complexes containing an axial phosphine oxide ligand: Field-induced single-ion magnetism behavior of the Dy(III) analogues. *Inorg. Chem.* **2020**, *59*, 6603–6612. [CrossRef] [PubMed]
13. González, A.; Gómez, E.; Cortés-Lozada, A.; Hernández, S.; Ramírez-Apan, T.; Nieto-Camacho, A. Heptacoordinate tin (IV) compounds derived from pyridine Schiff bases: Synthesis, characterization, in vitro cytotoxicity, anti-inflammatory and antioxidant activity. *Chem. Pharm. Bull.* **2009**, *57*, 5–15. [CrossRef] [PubMed]
14. Fondo, M.; Corredoira-Vázquez, J.; García-Deibe, A.M.; Gómez-Coca, S.; Ruiz, E.; Sanmartín-Matalobos, J. Dysprosium-based complexes with a flat pentadentate donor: A magnetic and ab initio study. *Dalton Trans.* **2020**, *49*, 8389–8401. [CrossRef]
15. Llunell, M.; Casanova, D.; Cirera, J.; Alemany, P.; Alvarez, S. *SHAPE: Program for the Stereochemical Analysis of Molecular Fragments by Means of Continuous Shape Measures and Associated Tools*; University of Barcelona: Barcelona, Spain, 2010.
16. Fondo, M.; Corredoira-Vázquez, J.; García-Deibe, A.M.; Sanmartín-Matalobos, J.; Herrera, J.M.; Colacio, E. Tb_2, Dy_2, and Zn_2Dy_4 complexes showing the unusual versatility of a hydrazone ligand toward lanthanoid ions: A structural and magnetic study. *Inorg. Chem.* **2018**, *57*, 10100–10110. [CrossRef] [PubMed]
17. Liu, J.-L.; Chen, Y.-C.; Tong, M.-L. Symmetry strategies for high performance lanthanide-based single-molecule magnets. *Chem. Soc. Rev.* **2018**, *47*, 2431–2453. [CrossRef]
18. Friedman, J.R.; Sarachick, M.P.; Tejada, J.; Ziolo, R. Macroscopic measurement of resonant magnetization tunneling in high-spin molecules. *Phys. Rev. Lett.* **1996**, *76*, 3830–3833. [CrossRef]
19. Thomas, L.; Lionti, F.; Ballou, R.; Gatteschi, D.; Sessoli, R.; Barbara, B. Macroscopic quantum tunnelling of magnetization in a single crystal of nanomagnets. *Nature* **1996**, *383*, 145–147. [CrossRef]
20. Ruiz, J.; Mota, A.J.; Rodríguez-Diéguez, A.; Titos, S.; Herrera, J.M.; Ruiz, E.; Cremades, E.; Costes, J.P.; Colacio, E. Field and dilution effects on the slow relaxation of a luminescent DyO9 low-symmetry single-ion magnet. *Chem. Commun.* **2012**, *48*, 7916–7918. [CrossRef]
21. Singh, A.; Shrivastava, K.N. Optical-acoustic two-phonon relaxation in spin systems. *Phys. Status Solidi B* **1979**, *95*, 273–277. [CrossRef]
22. Shrivastava, K.N. Theory of spin–lattice relaxation. *Phys. Status Solidi B* **1983**, *117*, 437–458. [CrossRef]
23. Day, B.M.; Guo, F.-S.; Layfield, R.A. Cyclopentadienyl ligands in lanthanide single-molecule magnets: One ring to rule them all? *Acc. Chem. Res.* **2018**, *51*, 1880–1889. [CrossRef]
24. Chilton, N.F.; Collison, D.; McInnes, E.J.L.; Winpenny, R.E.P.; Soncini, A. An electrostatic model for the determination of magnetic anisotropy in dysprosium complexes. *Nat. Commun.* **2013**, *4*, 2551. [CrossRef]
25. Armenis, A.S.; Bakali, G.P.; Brantley, C.L.; Raptopoulou, C.P.; Psycharis, V.; Cunha-Silva, L.; Christou, G.; Stamatatos, T.C. A family of mono-, di-, and tetranuclear Dy^{III} complexes bearing the ligand 2,6-diacetylpyridine bis(picolinoylhydrazone) and exhibiting slow relaxation of magnetization. *Dalton Trans.* **2022**, *51*, 18077–18089. [CrossRef]

26. Sasnovskaya, V.D.; Kopotkov, V.A.; Kazakova, A.V.; Talantsev, A.D.; Morgunov, R.B.; Simonov, S.V.; Zorina, L.V.; Mironov, V.S.; Yagubskii, E.B. Slow magnetic relaxation in mononuclear complexes of Tb, Dy, Ho and Er with the pentadentate (N_3O_2) Schiff-base dapsc ligand. *New J. Chem.* **2018**, *42*, 14883–14893. [CrossRef]
27. Sheldrick, G.M. *SADABS, Area-Detector Absorption Correction*; Siemens Industrial Automation, Inc.: Madison, WI, USA, 2001.
28. Sheldrick, G.M. Crystal structure refinement with SHELXL. *Acta Cryst.* **2015**, *C71*, 3–8.